



Synergistic hydrogen atom transfer with the active role of solvent: Preferred one-step aerobic oxidation of cyclohexane to adipic acid by N-hydroxyphthalimide



Futong Liang, Wenzhou Zhong*, Liping Xiang, Liqiu Mao*, Qiong Xu, Steven Robert Kirk, Dulin Yin

National & Local United Engineering Laboratory for New Petrochemical Materials & Fine Utilization of Resources, Key Laboratory of Chemical Biology Traditional Chinese Medicine Research Ministry of Education, College of Chemistry and Chemical Engineering, Hunan Normal University, Changsha 410081, PR China

ARTICLE INFO

Article history:

Received 19 April 2019

Revised 26 August 2019

Accepted 28 August 2019

Keywords:

Cyclohexane

Adipic acid

Solvent effect

Aerobic oxidation

N-hydroxyphthalimide

ABSTRACT

In this work, we developed an one-step aerobic oxidation of cyclohexane to prepare adipic acid, catalyzed by N-hydroxyphthalimide (NHPI) under promoter- and metal-free conditions. A significant beneficial solvent effect for synergistic reaction is observed with varying polarity and hydrogen-bonding strength: detailed study reveals that the solvent environments manipulate catalytic activity and adipic acid selectivity. Cyclic voltammetry measurements and UV–visible spectra of the NHPI catalyst are examined in various solvent environments to understand the active role of solvent in influencing the catalytic-site structure ($>\text{NOH}$) of the molecule. Analysis of the UV–visible spectra reveals that these differences can be rationalized by considering hydrogen-bonding with solvent molecules, which modifies the catalytic-site structure. This observation is in agreement with cyclic voltammetry results: the different reversibility of the catalytic-site ($>\text{NOH}/>\text{NO}^\bullet$) wave shows that the catalytic activity of NHPI is related to the formation of hydrogen bonds with the active participation of solvents. Computational studies presented herein have furnished mechanistic insights into the effect of solvent environments. Specifically, we present the structures, dissociation energies, and reaction barriers from DFT studies of the reactants and reaction intermediates involved in the two types of H-abstraction on $>\text{NO}^\bullet$ catalytic-sites for the rate-determining step. The results of modeling the solvent effects using the PCM continuum solvent method predict that the resulting reaction barrier of the rate-controlling H-abstraction for cyclohexane and cyclohexanone is modified significantly: the transition state barrier of H-abstraction for cyclohexane decreases from 22.36 (in benzene) to 20.78 kcal·mol⁻¹ (in acetonitrile); the α -H-abstraction barrier for cyclohexanone decreases from 21.45 to 20.53 kcal·mol⁻¹. The active participation of solvent molecule results in a strong interaction between pre-reaction complex ($\text{PINO}\cdots\text{H}\cdots\text{C}<$) with the migrating hydrogen and polar solvent molecules, which in turn favors the H-abstraction by a hydrogen-transfer to the $>\text{NO}^\bullet$ catalytic-sites at the transition state. The lower calculated barriers of H-abstraction for cyclohexanone oxidation approximate more closely the experimental results of the higher adipic acid selectivity. Our work provides a dimension of sustainable chemistry for the metal-free preparation of adipic acid: a conversion of 27% with 79% adipic acid selectivity is achieved over use of NHPI catalysts in CH_3CN solvent.

© 2019 Elsevier Inc. All rights reserved.

1. Introduction

Selective aerobic oxidation of sp^3 hybridized carbon of non-activated alkanes is one of the “dream reactions” for transformation of petroleum-based feedstocks to various useful chemicals from the academic and industrial perspective [1–3]. Probably, apart from their high bond dissociation energy of $\text{C}(\text{sp}^3)\text{—H}$ bonds (90–100 kcal·mol⁻¹) for hydrogen-atom transfer in alkane activa-

tion [4], the O_2 molecule with a nominal double bond (1.208 Å) in its triplet ground state is also kinetically hindered to produce reactive species (O_2^+ , O_2^- , $\text{O}_2^{\cdot-}$, HO^\bullet , HOO^\bullet and H_2O_2) toward the strong $\text{C}(\text{sp}^3)\text{—H}$ bonds. To overcome this impediment, given that a high activation energy (e.g., high reaction temperature $>175^\circ\text{C}$) first has to be supplied for O_2 and $\text{C}(\text{sp}^3)\text{—H}$ bond activation, this hydrogen abstraction step by O_2 is even more exothermic. Thus, it is difficult to dissipate the reaction heat and stop the process at the stage of carboxylic acids to avoid overoxidation to CO_2 . For instance, direct aerobic oxidation of cyclohexane (with rather poor performance) produces adipic acid (AA), which is in turn used to

* Corresponding authors.

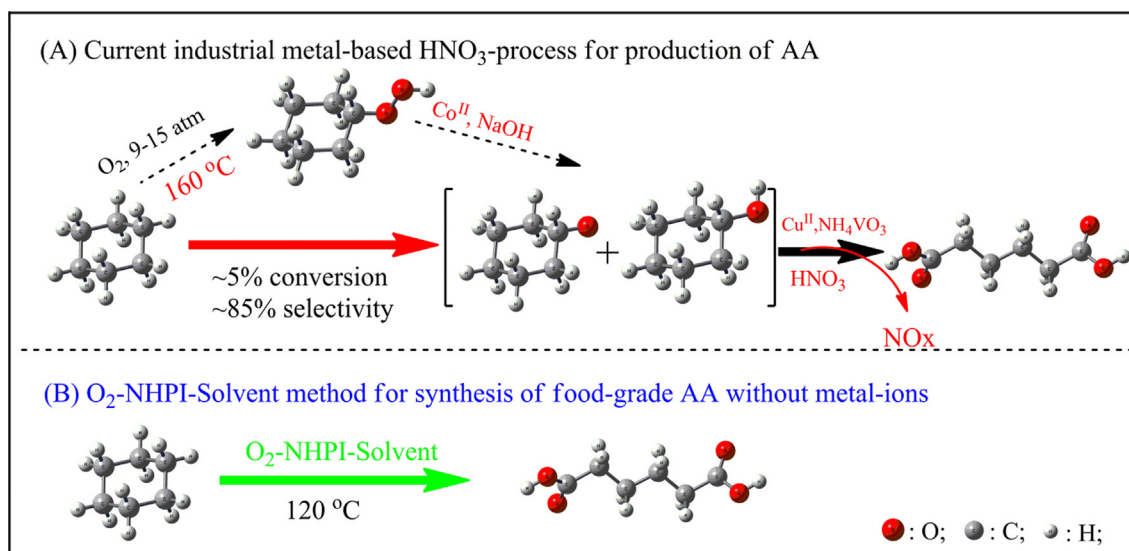
E-mail addresses: zwenz79@163.com (W. Zhong), mlq1010@126.com (L. Mao).

prepare Nylon-66 polymers and pharmaceutical intermediates. At present, the industrial conversion of cyclohexane to AA undergoes a two-step process involving the Co-catalyzed autoxidation of cyclohexane at 150–180 °C to a KA-oil (a mixture of cyclohexanone and cyclohexanol) and the nitric acid oxidation of the KA-oil to AA [5,6]. The main drawbacks of this process are that the aerobic oxidation in the first step must be operated with less than 4% cyclohexane conversion to keep a high KA-oil selectivity (70–80%), and that the nitric acid oxidation in the second step produces a large amount of undesired global-warming substances like N_2O (Scheme 1) [7,8]. An extensive body of research on bioderived feedstocks has been directed at alternative processes of AA synthesis: these processes, however, require multiple chemical conversions and/or employ transition-metal catalysts [9,10]. The direct C–H bond functionalization of cyclohexane to AA with O_2 has therefore emerged as a promising approach to molecular construction with high atom- and step-economy in industrial chemistry.

Recently a great number of interesting aerobic cyclohexane oxidation processes to AA have been achieved by using transition-metal catalyst, because the aforementioned hurdles can be overcome by use of a redox-active metal to activate both O_2 and the C–H bond. For the first time, by applying a high concentration of Co^{3+} acetate combined with acetaldehyde as the promoter, Tanaka et al. succeeded in achieving conversion of cyclohexane to AA under 3 MPa oxygen pressure [11]. The patent described the cyclohexane oxidation with dioxygen using a novel system composed of a solvent-soluble cobalt salt and a chromium compound, with which a high AA selectivity of about 40% was attained [12]. Simonato et al. reported one-step process for obtaining AA from cyclohexane using a stable lipophilic carboxylic-acid with low manganese and cobalt salts loadings [13]. Lü and co-workers claimed an aerobic catalytic system for the direct production of AA from cyclohexane over the Anderson-type $[(C_{18}H_{37})_2N(CH_3)_2]_6-Mo_7O_{24}$ catalyst [14]. Molecular sieve catalysts with active-site metal isolation such as FeAlPO-31 and MnTS-1 have been designed for the direct oxidation of cyclohexane to AA [15,16]. In recent years, NHPI, a powerful carbon-radical-chain promoter, has been used as a valuable catalyst for the efficient aerobic oxidation of cyclohexane to AA in the presence of transition metal ions as co-catalysts under mild reaction conditions [17]. However, most of these catalytic systems are based on metal catalysts or co-catalysts, especially transition-metal ions such as Mn, Fe, Mo and

Co, which may possibly leave toxic traces of heavy metals in the product grades intended to satisfy food- and drug-grade specifications. In the context of metal-free catalysis, N-doped carbon materials were recently discovered active in the cyclohexane oxidation with <60% AA selectivity [18–21]. The development of metal-free catalytic systems for the efficient oxidation of cyclohexane to AA therefore appears appealing from the perspective of sustainable and green chemistry, which still remains a scientific challenge.

The direct aerobic oxidation of cyclohexane to AA proceeds according to a widely known free radical chain mechanism, where the elementary reaction results in homolysis not only of the desired C–H bonds but also of undesired C–C bonds (a lower bond energy). More importantly, the free radical mechanism suffers from a major limitation imposed by its intrinsic nature: the C–H bond of reaction products is very often more reactive than the starting material and formed intermediate [22]. In the past several years, a unique phthalimido-N-oxyl (PINO \cdot) radical from NHPI has been introduced to the aerobic oxidation process which enhances the initiation and propagation steps in the autoxidation cycle [23–27]. It is demonstrated that there is an established equilibrium $ROO\cdot + NHPI = ROOH + PINO\cdot$, where the reverse reaction is very fast. Thus, in order to shift the equilibrium right to form more PINO \cdot , a third component such as transition metals can be added to reduce the ROOH concentration, since the PINO \cdot radical is more reactive than the ROO \cdot counterpart in abstraction of the C–H bond hydrogen [28]. Interesting, some nonmetallic organic substrates and reaction intermediate such as alcohol, aldehyde, ketone, acid and AIBN, have recently been used as mediators combined with NHPI for ROOH activation by abstracting a hydrogen [29–32]. In contrast, regarding the metal-free method, the fact that organic solvents can play critical active roles in NHPI and ROOH activation during the elementary reaction step though their effects of electronic structure on the oxidation is, however, often ignored. At present, organic solvent is usually considered to be a reagent for the dissolution of NHPI [17]. Probably because catalytic system is the presence of co-catalysts or promoters, the synergistic nature of the solvent-NHPI interface for hydrogen atom transfer (HAT) appears to be of little importance for aerobic cyclohexane oxidation to AA. For example, NHPI combined with $Mn(acac)_2$ and $Co(acac)_3$ in acetic acid is able to show specific catalysis for the formation of AA, where a selectivity up to 70% is obtained [33]. Therefore, any further understanding of the synergistic catalytic



Scheme 1. Comparison of current industrial process and green method presented herein for production of AA.

performance of solvent would be impossible without detailed unravelling of the solvent effects alone for the NHPI-based catalytic system (without the presence of any co-catalysts or promoters) on the reactivity and AA selectivity in the aerobic cyclohexane oxidation.

Solvent-induced $C(sp^3)$ –H bond activation of alkane to produce active radicals can be an alternative to improve the catalytic oxidation process, avoiding the usage of organic promoters or transition-metal co-catalysts. Reported here is a novel observation of the synergistic catalytic function of solvent as an independent organic promoters or transition-metal co-catalysts for NHPI-catalytic oxidation of cyclohexane to AA with dioxygen. In the absence of any co-catalyst, these experiments are carried out for the NHPI-catalytic aerobic oxidation of cyclohexane, also including linear paraffin in different solvents. The obtained data provide a rigorous assessment of HAT features in terms of the relative cyclohexane reactivity and AA selectivity in different solvents. The synergistic effect of CH_3CN and NHPI ensures its efficient catalytic ability: 27% cyclohexane conversion with 79% selectivity for AA can be achieved at 120 °C under 1.0 MPa of dioxygen in 6 h. Theoretical calculations by DFT (density functional theory) with the PCM continuum model are made to gain important information on the structures, dissociation energies, and reaction barriers of the reactants and intermediates involving in the two types of H-abstraction on $>NO\cdot$ catalytic-sites of $PINO\cdot$ for solvent activation, which further entitles us to propose possible rate-determining elementary reaction steps based on the catalytic action of NHPI alone. The synergistic catalytic function of solvent disclosed in this study will not only shake the understanding of the solvent as an active participant (not a reagent for only the dissolution of NHPI) in earlier NHPI-metal catalysis process, but also provides a new dimension of sustainable chemistry for the metal-free preparation of AA.

2. Experimental

2.1. Characterization techniques

Cyclic voltammetry is performed using a three-electrode configuration and an autolab electrochemical workstation (Eco Chemie, Holland). The working electrode (WE) is a glassy carbon electrode (GCE, 3-mm diameter disk), the counter electrode is a graphite rod and the reference electrode is a KCl saturated calomel electrode (SCE). All the measurements here are carried out at room temperature (25 °C) under argon atmosphere, and all potentials are reported vs the SCE. The UV–visible spectra of liquid samples are recorded on a UV-2450 spectrophotometer (Shimadzu, Japan). The solvent is measured as a reference/background spectrum.

2.2. DFT calculations

All calculations are done within Gaussian 09 software [34] based on the B3LYP/6-311++G(2df, 2pd) level of theory, which has been widely used in the theoretical studies on the aerobic oxidation promoted by hydroxyimide catalysts [32,35,36]. To explore the effect of solvent for the key elementary step by NHPI catalysts, all geometry optimizations and vibrational frequency analyses of the reactants, pre- and post-reaction (noncovalently bound) complexes, and the cisoid transition state (TS) structures are performed with the solvation effect included using the PCM solvation model. All non-TS structures are verified to have only positive vibration frequencies, and the TS structures have a single imaginary frequency that lead to the corresponding pre- and post-reaction species. The liquid-phase bond dissociation energies (BDEs) calculations in different solvents make use of the bond dissociation

work reaction, which is demonstrated to give satisfactory results for such H-abstraction processes.

2.3. Catalytic oxidation of cyclohexane to AA by NHPI-solvent systems

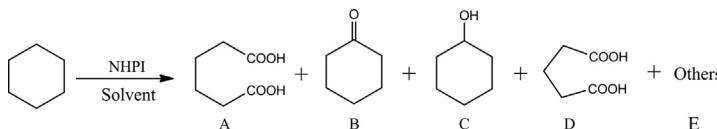
Liquid phase catalytic oxidations were carried out in a Teflon-lined 100 mL stainless steel reactor equipped with a magnetic stirrer. Typically, 3.2 g of cyclohexane, 6.4 g of solvent and 0.6 g of NHPI catalyst were charged in the autoclave, and then heated to the reaction temperature (120 °C) under magnetic stirring (800 rpm). Oxygen was then charged into the reactor to the desired pressure (1.0 MPa). The reaction was terminated by switching off the stirrer and immediately cooling the reactor in an ice-water bath. The reaction mixture was dissolved in ethanol and filtered. The components of the liquid phase such as unreacted cyclohexane and KA-oil intermediate were quantitatively analyzed on a Shimadzu 2010 plus gas chromatograph with a DB-17 polysiloxane capillary column (30 m × 0.32 mm × 0.50 μm) and flame ionization detector (FID) using chlorobenzene as the internal standard. The injector and detector temperature were 250 °C, and the column temperature was 100 °C. The yield of cyclohexanol was calculated as a difference between the value obtained by GC and the concentration of cyclohexyl hydroperoxide determined iodometrically (reduction in cyclohexyl hydroperoxide with PPh_3 gives an additional amount of cyclohexanol). The AA and overoxidation products (succinic acid, glutaric acid and valeric acid) were quantitatively analyzed according to the external standard method using an Agilent 1200 series high-performance liquid chromatography instrument equipped with a UV detector (Agilent G1365B MWB) and a column of Zorbax Eclipse XDB C18 (150 mm × 4.6 mm i.d.). The eluent was 0.01 mol/L KH_2PO_4 in a 1:9 methanol/water mixture and a flow rate set at 1.0 mL/min, and ultraviolet detector set at 212 nm. To detect possible components of oxygen formed, the gases in the reactor were also collected with a gas bag after termination of the reactions and then analyzed by gas chromatography with a TCD detector. The products were satisfactorily identified by comparing the MS spectra with those of the authentic samples. In addition, after the solvent was removed under reduced pressure, the isolation of AA on a preparative scale is carried out as the following procedure. Acetonitrile (20 mL) was added to the reaction mixture to give a white solid. After filtration, 0.64 g of AA was obtained.

3. Results and discussion

3.1. Active role of solvent on NHPI-catalyzed aerobic oxidation of cyclohexane

In studying solvent effects, the solvent molecule has perhaps too often been regarded as a continuous medium rather than as an active participant in the catalytic reaction. In what follows, the oxidation of cyclohexane to AA is chosen as a model reaction to investigate the active role of solvent on NHPI-catalyzed aerobic oxidation of hydrocarbons, and the central feature of the approach is envisioned to arise from the two types of H-abstraction (cyclohexane and cyclohexanone) on $>NO\cdot$ catalytic-sites of $PINO\cdot$ for the rate-determining step [37]. Therefore, the active participation of a solvent in the reaction is of direct interest for us in this work to elucidate the solvent specificity on one-step oxidation of cyclohexane to AA in the absence of transition-metals as co-catalysts. The active roles of different solvents are examined in the oxidation of high-concentrated cyclohexane to four main products (cyclohexanone, cyclohexanol, AA and glutaric acid) at 120 °C under 1.0 MPa O_2 for 6 h. As shown in Table 1, the blank run without solvent using NHPI alone gave the traces of cyclohexyl hydroperoxide

Table 1
Direct aerobic oxidation of cyclohexane to AA catalyzed by metal-free NHPI-solvent systems.^a



Entry	Solvent	Conv. ^b (%)	TON ^c	Selectivity ^d (%)				
				A	B	C	D	E
1	Without	trace	–	–	–	–	–	–
2	Pyridine	trace	–	–	–	–	–	–
3	Acetone	28.5	2.85	56.7	31.2	3.9	7.0	1.2
4	Ethanol	8.3	0.83	13.1	36.5	49.4	–	1.0
5	Acetic acid	21.6	2.16	79.1	13.5	2.4	4.8	0.2
6	Benzonitrile	7.3	0.73	9.4	67.6	21.1	–	1.9
7	Propionitrile	19.9	1.99	67.4	18.5	5.1	8.0	1.0
8	Acetonitrile	27.4	2.74	79.4	9.3	3.4	7.1	0.8
9	Benzene	1.8	0.18	–	72.2	26.1	–	1.7
10	Dichloromethane	1.7	0.17	11.3	73.4	12.4	0.1	2.8
11	H ₂ O	trace	–	–	–	–	–	–
12	Trifluoroethanol	26.1	2.61	60.9	12.7	4.2	16.3	5.9
13 ^e	Acetonitrile	22.8	2.28	70.3	15.6	4.1	5.7	4.3
14 ^f	Acetonitrile	23.1	2.31	44.9	45.0	5.3	1.4	3.4
15 ^g	Acetonitrile	23.2	2.32	48.0	40.8	5.2	2.4	3.6
16 ^h	Acetonitrile	0.1	0.01	–	92.1	7.3	–	0.6
17 ⁱ	Acetonitrile	33.8	3.38	28.1	68.4	–	–	3.5
18 ^j	Acetonitrile	56.5	5.65	74.1	–	–	–	25.9

^a All reactions were done with 0.6 g of catalyst, 3.2 g cyclohexane, 6.4 g of solvent, at 120 °C, under 1.0 MPa, time (6 h).

^b Conversion (%) based on substrate = $(1 - [(concentration\ of\ substrate\ left\ after\ reaction) \times (initial\ concentration\ of\ substrate)^{-1}]) \times 100$.

^c Turnover number (TON): number of moles of cyclohexane converted per mole of NHPI catalyst.

^d Product selectivity = content of this product/(adding cyclohexane amount (mmol)-the amount of cyclohexane recovered (mmol)) \times 100%; Others: cyclohexyl peroxide, 2-hydroxycyclohexanone, 4-hydroxycyclohexanone and 1,2-cyclohexanedione, ϵ -caprolactone and succinic acid.

^e Adding Mn(OAc)₂ (0.04 g).

^f Adding Co(OAc)₂ (0.04 g).

^g Adding butyl ketone oxime (0.34 g).

^h Adding hydroquinone (0.21 g).

^{i, j} Using cyclohexanone or cyclohexanol (3.2 g) instead of cyclohexane.

product (entry 1). In addition, the blank test using NHPI-free CH₃CN solution for the reaction detects no cyclohexane consumption, indicating no reaction of cyclohexane in the absence of NHPI catalysts (not shown). Surprisingly, it is found that NHPI in combination with CH₃CN solvent realized 27.4% conversion of cyclohexane with the selectivities of 79.4% for AA, 9.3% for cyclohexanone, 3.4% for cyclohexanol and 7.1% for glutaric acid (entry 8). However, under different conditions similar to those used in Refs. [30,38]. (80 °C, 1 atm O₂, cyclohexane in CH₃CN with NHPI as catalyst), the co-presence of transition-metals significantly change the product selectivity, and the highest selectivity for cyclohexanone is obtained. When acetic acid, its with fairly high polarity, is used in place of CH₃CN in this oxidation, cyclohexane can also be one-step converted efficiently to AA (79.1%) at a slightly lower conversion of 21.6% under our experimental conditions (entry 5), which is similar to previous transition-metals/NHPI system [17]. The same observation holds true for oxidation of cyclohexane in acetone, which shows a good active role with fairly extensive cyclohexane conversion (28.5%), while the selectivity of cyclohexane to AA is decreased from 79.4% to 56.7% (entry 3). In addition, other solvents such as ethanol and benzene (entries 4 and 9) are examined and, unlike an ethanol environment which gives 8.3% conversion (13.1% AA selectivity), benzene shows no formation of AA with less than 2% conversion. The above results clearly reveal that there must be some synergistic active effects of a unique polar solvent to significantly promote the NHPI-catalyzed aerobic direct oxidation of cyclohexane to AA.

In the literature, several organic compounds such as aldehydes and α, α -azoisobutyronitrile for mediation of the NHPI-based aero-

bic oxidation have been reported and in most of the cases the reaction proceeds via a radical mechanism. Similar to transition-metal co-catalysts, these organic mediators play the sole role of a radical initiator to induce the formation of PINO[•] from NHPI. According to the reported literature [39,40] and our experimental observations, we believe that our solvents also have the same mediation effect, where the rapid decomposition of cyclohexyl hydroperoxide intermediate to form a radical initiator for NHPI is promoted by the interaction of cyclohexyl hydroperoxide with the solvent molecule. Thus, the rapid increase of PINO[•] free-radicals promotes the propagation of free-radical reactions. Meanwhile, oxidative attack on the C–H bond of another cyclohexane or cyclohexanone, assisted by the hydrogen-bond interaction with solvents may be more easily to be captured by PINO[•] free-radical for the formation of AA via β C–C bond cleavage. In order to further confirm whether the presence of the solvent hydrogen-bond promotion effect in the NHPI-based catalytic system is responsible for the good catalytic performance in the oxidation, non-hydrogen-bonded dichloromethane solvent is added to this catalytic system to replace CH₃CN. The solution of dichloromethane gave rather low conversions of 1.7%, and the AA selectivity decreased from 79.4% to 11.3% (entry 10). As a result, these observations suggest the testable hypothesis that a hydrogen-bonded solvent can assist the decomposition of cyclohexyl hydroperoxide and the activation of C–H bond by modifying the bond dissociation energies and reaction barriers, thereby resulting in an increased catalytic activity. To verify this hypothesis, we investigated the same reaction with the addition of tiny amounts of solvents (equimolar ratios with the NHPI unit) to the oxidation solution, instead of working with

large amounts of solvents (Table S1). An analogous beneficial effect is also observed in terms of both cyclohexane conversion and AA selectivity (compare between Table S1 and Table 1), when operating with the hydrogen-bonded solvents. Notably, however, oxidations carried out in the presence of small amounts of non-hydrogen-bonded solvents in solution, did not show any further increase in cyclohexane conversion, confirming again the activation role of hydrogen-bonded solvents to fully promote the HAT process.

In order to further address these questions, we introduce three analogs of CH_3CN as solvent by substituting the methyl group with an ethyl or phenyl group, respectively. The different functional groups in propionitrile have a similar α -H atom from the alkyl group, but electronic effects may be different for various H-abstraction elementary reactions in the comparison of the bridging of $-\text{CH}_3$ for CH_3CN . Benzonitrile, without an α -H atom, can be a control used to probe the environmental hydrogen-bond interaction, which may be bound by reaction intermediates. In Table 1, it is seen that as the chain length of the primary nitriles increased (entries 7 and 8), the rate of reaction and AA selectivity became significantly lower under the same conditions. In contrast, benzonitrile leads to a pronounced decrease in the catalytic activity for cyclohexane conversion (from 27.4% to 7.3%). Meanwhile, AA selectivity clearly displayed opposite trends as compared to CH_3CN , where interestingly 9.4% selectivity of AA along with KA-oil (ketone/alcohol = 3.2) at 88.7% selectivity is observed (entry 6). As a benchmark, the catalytic reaction was carried out in pyridine as a solvent, and low conversions of below 0.1% were obtained, demonstrating that the α -H atom of solvents may play a positive role in a hydrogen-bonding interaction for enhancing catalytic activity. Interesting, transition metals salts ($\text{Mn}(\text{OAc})_2$ and $\text{Co}(\text{OAc})_2$) or organic additives (diacetylmonoxime) are known to pull hydrogen out from organic compounds forming radicals and/or to promote the decomposition of peroxide species in the NHPI-based catalytic system [37]. However, these additives have negative influences on the catalytic activity and AA selectivity under our experimental conditions (entries 13–16). In addition, in order to confirm whether solvent polarity has a key role on the β -scission in formed alkoxy radicals for the formation of AA with the reaction being strongly accelerated by polar solvents in catalytic system, several commonly used solvents such as H_2O and 2,2,2-trifluoroethanol were added (Table 1, entries 11 and 12) [41]. The reaction with H_2O solvent did not proceed well, which give trace results. This suggested that the activation role of the polar solvent should be likely involved in the HAT process by stabilisation of the transition state with the favorable intermolecular hydrogen-bonding interactions (with certain solvents), which is consistent with previous results in this area [22,42].

The CH_3CN -NHPI reaction system presents the highest catalytic efficiency for the one-step synthesis of AA, so we investigated the effect of reaction parameters (Fig. 1). The solvent effect of changing the cyclohexane concentration is studied and the results are shown in Fig. 1A. It is observed that with an increase in the cyclohexane concentration, initially the cyclohexane conversion increases continuously (till 2.0 mol/L), but after 2.0 mol/L the conversion of cyclohexane decreases. The product selectivity of cyclohexane oxidation is also dependent on the cyclohexane concentration (solvent content); the AA selectivity gradually increases with increasing cyclohexane content and reaches a maximum in the cyclohexane concentration of 4.7 mol/L, whereas the selectivity to KA-oil intermediate rapidly decreases. This is easily understandable, as the 'cage' effect of the highly-concentrated solvent would reasonably be regarded as the inhibiting factor for further oxidation of KA-oil to AA [43]. The use of cyclohexane in large excess for increasing cyclohexane oxidation catalysis may, however, not be a proper strategy due to the formation of a two-phase system

with the limit of mass transfer. The NHPI amounts on the promotion effects of the solvent towards the cyclohexane conversion are shown in Fig. 1B. The results reveal that the conversion and AA selectivity increase in the CH_3CN solution with an increase in the amount of NHPI. However, the conversion and selectivity for AA are lowered to 24.5% and 73.5%, respectively, when the NHPI amount is increased to 1240 mg. Maybe partial NHPI catalyst (at the high concentration) is easy to form dimeric adducts (or higher aggregates) by a self-coordination of hydrogen-bond acceptor ($\text{C}=\text{O}$) and donor ($\text{N}-\text{OH}$) groups of NHPI, which leads to NHPI deactivation [32]. The aerobic oxidation results at different temperatures, pressures and time are also shown in Fig. 1. With the reaction temperature rising from 80 to 120 °C, the cyclohexane conversion increases with the concomitant gradual increase of AA and also of KA-oil selectivity (Fig. 1C). A similar reaction trend is also observed with the reaction pressures rising from 0.6 to 1.0 MPa (Fig. 1D). These results clearly indicate that cyclohexane is first converted into KA-oil intermediates and then further converted into AA, and that reaction energy and oxygen concentration have a significant effect on the oxidative cleavage of KA-oil at a higher temperature and pressure. On increasing reaction pressure to 1.2 MPa or raising the temperature to 130 °C, the catalytic efficiency of CH_3CN -NHPI doesn't change significantly, while degradation rate of AA increased rapidly. It is well observed that the cyclohexane conversion increases with prolonging time (Fig. 1E) but the selectivity of AA first increases and then decreases due to occurrence of AA degradation by deep oxidation at the too much elongated reaction time.

3.2. Oxidation of various hydrocarbons by CH_3CN -NHPI system

The metal-free aerobic oxidation by the NHPI- CH_3CN catalytic system provides a sustainable one-step route to AA, although the catalytic oxidation of cyclohexane by transition-metal/NHPI leads to an AA as a main product along with a mixture of KA-oil. With the optimized reaction conditions, this metal-free catalytic system can be extended to catalyze the oxygenation of various hydrocarbons (Table S2). Firstly, we test cycloalkanes to the corresponding dicarboxylic acids. Cyclopentane is oxidized with 18.6% conversion and 70% selectivity of glutaric acid under the same conditions (entry 1). 66.5% of cyclooctane is also compatible, affording the desired acid products with 53.2% selectivity (entry 2). In addition, we have also explored the oxidation of linear alkanes. N-Pentane can give rise to the pent-2-one with 43.6% selectivity, along with pentan-3-one (34.6%, entry 3). 37.6% N-hexane, 31.3% N-heptane and 40.3% N-octane can also be transformed into the corresponding oxidated products efficiently, respectively. However, about 17% propionic acid or valeric acid are formed as the carbon-carbon bond cleaved products by the cleavage of hexan-3-one or heptan-3-one and octan-4-one, respectively. Meanwhile, the mixed products such as 2-one, 3-one and 4-one are obtained with 50% total selectivity (entries 4, 5 and 6). The above results indicate that these cleaved products such as valeric acid, propionic acid and acetic acid seem to be formed via β -scission of the corresponding alkoxy radical derived from the alkyl hydroperoxide decomposition by solvent participation, which is similar to the previous transition-metal/NHPI catalytic system by metal ions as co-catalyst for the decomposition of alkyl hydroperoxide [43,44]. Usually, the extent of the β -scission is thought to be related to the alkoxy radicals stability. Therefore, the β -scission of a 2-oxy radical to form organic acid occurs more easily than that of a 3-oxy or 4-oxy radical. It is interesting that the higher catalytic efficiencies of the branched alkane such as 3-methyl pentane in CH_3CN solvent are found with 63.2% conversion, a β -scission of a 3-methyl-3-oxypentan radical to pentan-3-one as a major product (58.4%) along with 3-methylpentan-3-ol (19.0%) occurs (entry 7). One

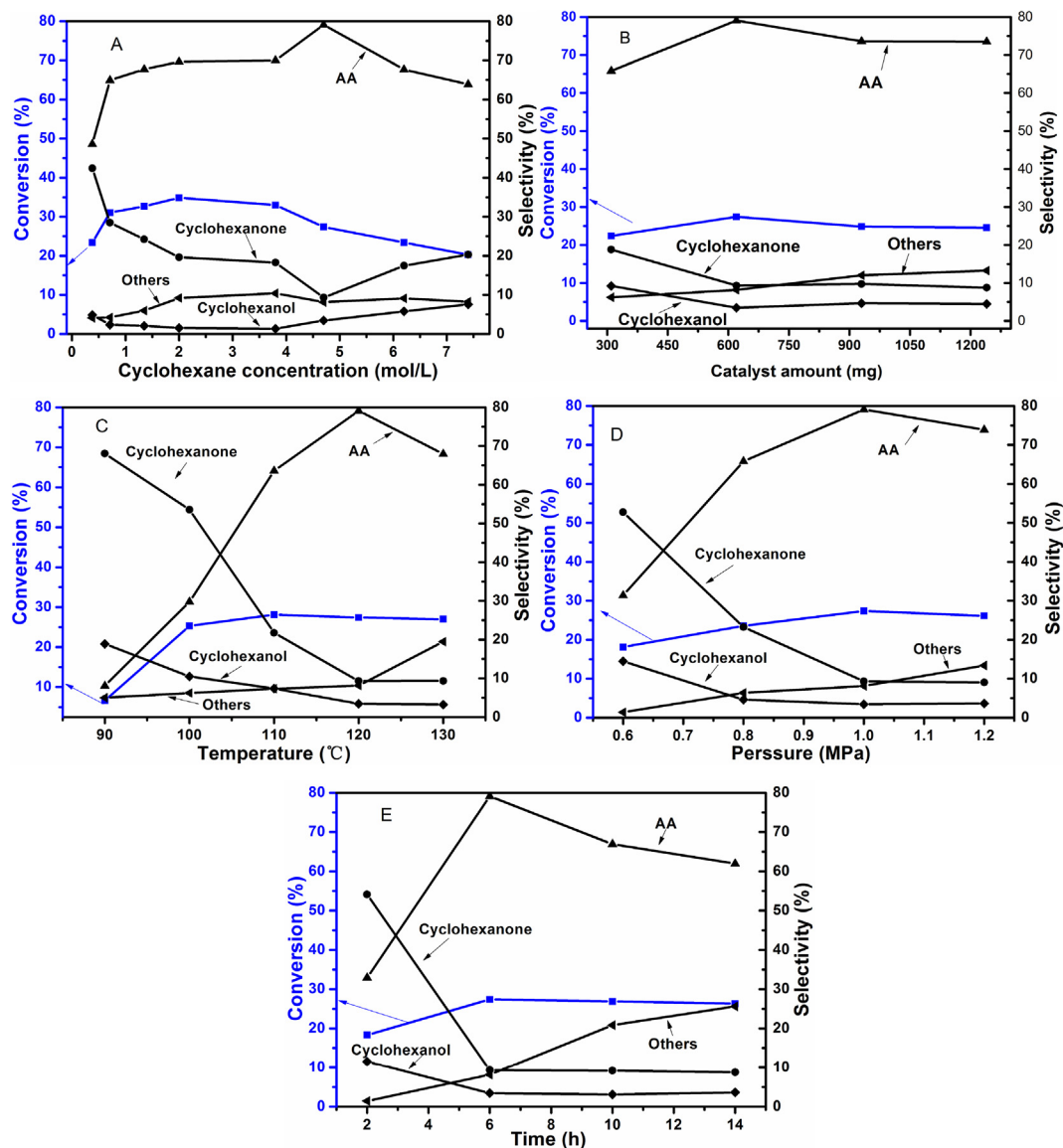


Fig. 1. Effect of the cyclohexane concentration (A), catalyst amount (B), temperature (C), reaction pressure (D) and time (E) on the conversion of cyclohexane and AA, cyclohexanol, cyclohexanone and glutaric acid selectivity over the CH_3CN -NHPI systems.

may envision that, for branched alkanes in CH_3CN , the β -scission of the tertiary-carbon oxy-radical occurs more easily than for the secondary-carbon oxy-radical; hence, both reactivity and cleaved product selectivity increase. Finally, we focused on alkylbenzene such as methylbenzene, ethylbenzene and cumene (entries 8, 9 and 10). The compounds with tertiary- and secondary-hydrogen atoms in alkyl groups can afford the corresponding acetophenone products in moderate to good selectivity. However, starting from methylbenzene the reaction proceeded with a slower rate, probably because of a higher primary C–H bond energy. It should be noted that tertiary hydrogen attraction is indeed favored and, after 6 h, a 84% conversion is obtained. The formation mechanism of the acetophenone product is similar to 3-methyl pentane, in which the β -scission of tertiary-carbon oxy-radical occurs easily under reaction conditions.

3.3. Characterization results

Identical amounts of NHPI catalyst in different solvents were examined by UV–visible spectroscopy (Fig. 2A), and the distinctly

identifiable spectrum of NHPI is evolved. NHPI catalysts in CH_3CN and $\text{C}_2\text{H}_5\text{CN}$ show a very intense electronic transition near 232 nm, and the greater number of hydrogen-bond interactions of CH_3CN and $\text{C}_2\text{H}_5\text{CN}$ as an electron-accepting molecule lead to a new electronic transition due to the change in the HOMO–LUMO energy gap. This assertion is supported by the following facts: a similar electronic transition at 250 nm is observed in CH_3COOH solvent, but is weak. However, in pyridine and $\text{C}_6\text{H}_5\text{CN}$, NHPI shows a red absorption in the 350 nm [39], which probably originates from a weak self-coordination of hydrogen-bond acceptor (C=O) and donor (N–OH) groups of NHPI into dimeric adducts (or higher aggregates) in absence of hydrogen-bond interaction with the solvents. A similar phenomenon was also observed by Cametti *et al.*, on lipophilic NHPI derivatives in apolar solution, with the >NO–H bond being directly involved in the self-aggregation process [32]. This suggests that the formation of dimeric adducts in absence of hydrogen-bond interaction with solvent might impede hydrogen atom transfer for the rate-determining step as shown in the above catalytic results of Table 1. In addition, the UV–visible spectra of a 15.2 mM 19.9% cyclohexane solution of cyclohexyl hydroperoxide

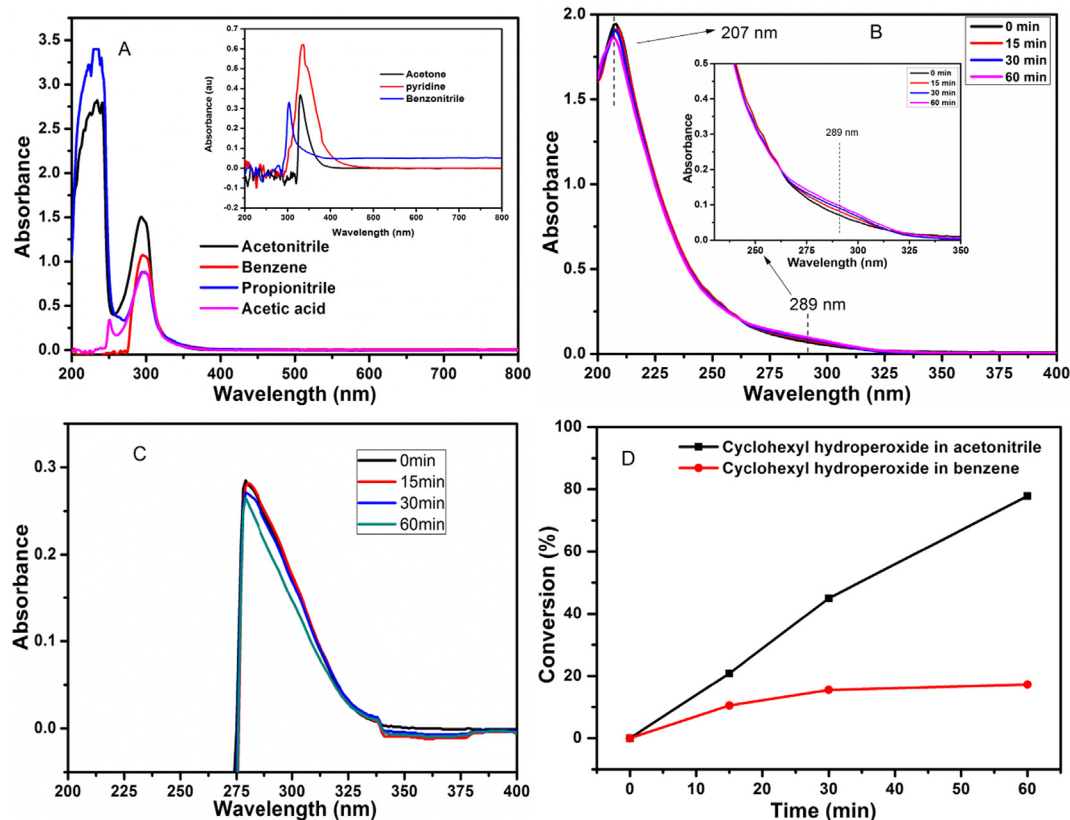


Fig. 2. UV-vis spectra (A) of NHPI in different acetic acid, acetonitrile, propionitrile and pyridine solvents (Inset is the UV-vis spectra of NHPI in acetone, benzene and benzonitrile solvents, $1.0 \times 10^{-3} \text{ mol}\cdot\text{L}^{-1}$); UV-vis spectra of cyclohexyl hydroperoxide in CH_3CN (B) and benzene (C) solvents for the different heating time at 100°C ; the decomposition rate of cyclohexyl hydroperoxide in CH_3CN and benzene (D).

in CH_3CN and that in benzene are different. An electronic transition at 207 nm is observed for cyclohexyl hydroperoxide in CH_3CN (see in Fig. 2B). Moreover, the strength of the peak decreases with increasing time at 100°C , illustrating that the heating induces the homolytic cleavage of the O–O bond of cyclohexyl hydroperoxide. On the other hand, the absorbance near 289 nm becomes gradually stronger with time, which is indicative of the formation of cyclohexanone. For comparison, in benzene solvent the spectra change more obviously and the O–O bond of cyclohexyl hydroperoxide are observed at 279 nm, where no formation of the hydrogen-bond has been proposed. Interestingly, this band does not change upon prolonging the heating time (till 0.5 h) at 100°C (Fig. 2C), which clearly shows by the fact that the decay of cyclohexyl hydroperoxide decomposition is very much slower when the CH_3CN is replaced by benzene (similar to the decomposition rate of cyclohexyl hydroperoxide in CH_3CN and benzene, respectively, as shown in Fig. 2D). These observations indicate that the homolytic cleavage of the O–O bond of cyclohexyl hydroperoxide can be strongly accelerated in the presence of the hydrogen-bond interaction with the solvent [43], in line with the occurrence of aerobic cyclohexane oxidation process.

Cyclic voltammetry (CV) measurements of the NHPI catalysts in the different solvent media are carried out to allow for the determination of the solvent-promotion effect. The CVs of NHPI (Fig. 3A) in the different media are different from each other, indicating that the catalytic oxidation process is significantly influenced by the solvent media. Notably, the CVs of the NHPI catalysts in acetonitrile and acetone exhibit a strong anodic peak at E_{pa} assigned to the one-electron oxidation of the $>\text{NOH}$ moiety for NHPI resulting in the nitroxide radical $>\text{NO}\cdot$; the reduction of the electrogenerated radical occurring on the reverse scan at E_{pc} .

The presence of a reduction peak confirms that the formed nitroxide radical $>\text{NO}\cdot$ is very stable in these solvent-based systems. By comparison with acetone, a negative shift in the oxidation peak potential of NHPI is also observed in the CVs in CH_3CN (from 0.990 V of acetone to 0.904 V of acetonitrile), as well as in the CVs conducted in propionitrile. These shifts in a negative direction can be attributed to the deprotonation of NHPI by the solvent containing N atom as a base to easily give the NHPI-anion, then the anion can be oxidized quickly on the electrode at 0.904 V to give the PINO \cdot radical ($>\text{NO}\cdot \rightleftharpoons >\text{NO}^{\ominus} \rightleftharpoons >\text{NO}\cdot$). In addition, the large ΔE_{p} ($E_{\text{pa}} - E_{\text{pc}}$) value in acetone (0.171 V vs 0.152 V) is observed due to the coupling of the deprotonation step with the difficulty in acidic medium and of the electron transfer for the electrogenerated radical cation which is a strong acidic species according to $>\text{NOH}^{\ominus} \rightleftharpoons >\text{NOH}^{\oplus} \rightleftharpoons >\text{NO}\cdot + \text{H}^+$ [45]. Hence, these shifts in a negative direction are in line with the ΔE_{p} value of the $>\text{NOH}/>\text{NO}\cdot$ redox couple in different media. Interestingly, very large catalytic currents are observed in the CVs of NHPI for acetonitrile (compare their height with the peak current of the one-electron $>\text{NOH}/>\text{NO}\cdot$ wave), suggesting that NHPI in CH_3CN is more reactive toward cyclohexane oxidation, which has also been observed for the similar systems by other authors [46]. In contrast, there is also a dramatic reduction of the catalytic current for acetic acid medium (compare the current heights of the CVs for NHPI-acetonitrile system), indicating that the less the oxidizing character of the catalyst (i.e. the driving force), the less efficient the catalytic process. Further, the usage of benzonitrile without an α -H atom, to replace the analog CH_3CN , where a low catalytic current is observed, alters the reversibility of the $>\text{NOH}/>\text{NO}\cdot$ wave, showing that the catalytic activity of NHPI is related to the formation of hydrogen bonds with

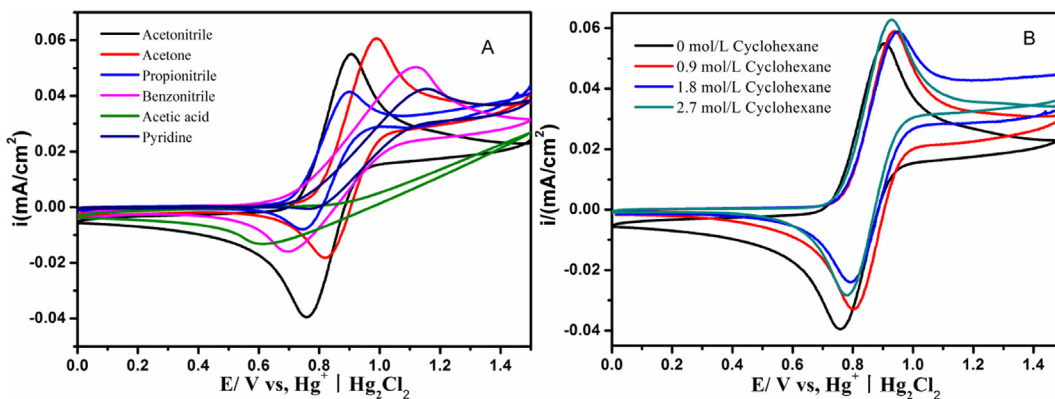


Fig. 3. Cyclic voltammograms of NHPI in different solvents (A) and NHPI in CH₃CN (3 × 10⁻³ mol L⁻¹) containing the different amounts of cyclohexane (B); Tetraethylammonium perchlorate served as the supporting electrolyte.

participation of the α -H atom between CH₃CN (a good hydrogen-bond-accepting solvent) and the hydroxyl proton of NHPI. Thus, the NHPI in CH₃CN can behave as redox catalysts, and carry out subsequent reactions that regenerate their reduced forms in the presence of cyclohexane.

Fig. 3B displays the variations of the CVs and the peak current as a function of the concentration of cyclohexane. Upon addition of cyclohexane, an enhancement of the anodic peak and a decrease of the cathodic peak are observed, indicating that the concentration of cyclohexane can influence the catalytic process kinetics. The peak current, i_p , is normalized toward the peak current; i_p^0 corresponds one electron $>NOH/>NO\cdot$ wave in the absence of cyclohexane [46,47]. Notably, it is observed that the i_p/i_p^0 and $(E_{pa} + E_{pc})/2$ values increase with the cyclohexane concentration, reaching a limiting value at high concentrations. Up to 2.7 mol/L cyclohexane, the $(E_{pa} + E_{pc})/2$ value is decreased, independent of i_p/i_p^0 , which is expected when the cyclohexane is in large excess over the NHPI catalyst and catalysis is not too fast so that the cyclohexane concentration across the reaction layer is the same as its bulk concentration. Thus, the enhancement of cyclohexane concentration triggers a dramatic increase of the catalytic efficiency, which is in agreement with the above catalytic results of NHPI with the different cyclohexane concentration. However the use of cyclohexane in large excess for increasing cyclohexane oxidation catalysis may not be a proper strategy due to the limit of mass transfer.

3.4. Mechanistic insights into these H-abstraction processes by theoretical calculation

Possible molecular mechanisms for the cyclohexane oxidation reactions in different solvents with NHPI as the metal-free catalyst are investigated using DFT calculations. First, the structural changes with the solvent interactions on the H-abstraction reactiv-

ity are explored by collecting the key geometrical and electronic properties of NHPI and its nitroso radical (Table 2). The $>NO-H$ bond lengths of NHPI in the polar solvents are larger than those in the gas conditions and apolar solvents, which was similar to the theoretical results for aerobic oxidation of alkylaromatics by using a lipophilic N-hydroxyphthalimide [36]. The longest $>NO-H$ bond is obtained in CH₃CN solvent. Similar trends in natural bond orbital (NBO) charge on the H atom are also found for the solvent active-effects, where the H_{NBO} in CH₃CN solvent has a larger NBO value than in apolar solvents. It was observed that their O–H BDEs are quite in line with their bond lengths and H_{NBO} . The O–H bond BDE values of NHPI in the polar solvents are somewhat lower than those in the apolar solvents. Specifically, the O–H BDE value in CH₃CN is the lowest among that of propionitrile and benzonitrile, which may be regulated by combining different substituting group linked –CN. Therefore, adding such protic solvents may alter the key geometrical and electronic properties of NHPI due to their favorable intermolecular hydrogen-bonding interactions with certain solvents, ultimately affecting the catalytic process. As a result, the catalytic behaviors for the aerobic oxidation of cyclohexane by NHPI catalysis vary in different solvents: NHPI in CH₃CN with the low O–H BDE and high H_{NBO} value thereby becomes much more reactive toward ROO \cdot . Compared with that of NHPI catalysts, the corresponding $>N-O$ bond of PINO \cdot in different solvents is shortened upon removing the O–H hydrogen atom from its precursor with the opposite trend, which is ascribed to the partial electronic delocalization of the nitrogen lone pair to the linked oxygen atom. Variable spin density distributions on the related O atoms are also caused by the solvent interactions with the following order: acetonitrile < propionitrile < benzonitrile < pyridine < acetic acid < acetone < benzene < cyclohexane < gas. Obviously, SD_{O_1} value of PINO \cdot in polar solvents not containing an N atom is larger than that in polar solvents containing an N atom, which can be ascribed

Table 2

The O–H, N–O bond lengths, O–H bond dissociation energies, atomic spin densities and NBO charges for NHPI and PINO \cdot in various solvents.

Solvent	ϵ	NHPI (N–O–H)				PINO \cdot (N–O)	
		O–H	O–N	p H	BED	p O	SD_{O_1}
Gas	–	0.96637	1.37072	0.475	84.162	–0.249	0.604086
Acetone	20.493	0.96846	1.36961	0.495	84.108	–0.299	0.572672
Acetic acid	6.2528	0.96805	1.36984	0.491	84.178	–0.289	0.579199
Acetonitrile	35.688	0.96855	1.36956	0.495	84.092	–0.301	0.571276
Propionitrile	29.324	0.96854	1.36941	0.495	84.097	–0.300	0.571691
Benzonitrile	25.592	0.96850	1.36958	0.495	84.101	–0.300	0.572027
Pyridine	12.978	0.96835	1.36976	0.494	84.129	–0.296	0.574474
Cyclohexane	2.0165	0.96720	1.37034	0.483	84.245	–0.267	0.592617
Benzene	2.2706	0.96734	1.37031	0.484	84.245	–0.270	0.590916

to the partial delocalization of the nitrogen lone pair of the solvent onto the radical oxygen atom due to their favorable intermolecular hydrogen-bonding interactions, thereby decreasing the corresponding spin densities located on the terminal O atoms of PINO \cdot . As a result, a smaller SD_O values would possess a stronger electron-withdrawing-like effect, indicating that they would have a higher H-abstraction reactivity. A similar trend of NBO charge for the O atom further supports the idea that the promotion effects of the solvent play a role in the hydrogen abstraction of the PINO \cdot radicals.

In addition, the generation of PINO \cdot from NHPI is also a vital step, as its overall catalytic efficiencies may not be correlated with its reactivity towards H-abstraction of cyclohexane or cyclohexanone. This may, however, facilitate the rapid formation of nitroxyl radicals that can efficiently propagate chains for longer, thereby boosting the reaction rate. As a result, the relative reactivity of the formation of a considerable amount of ROOH (Table 3) is evaluated in different solvents. The O–H BDE is 86.486–86.016 kcal \cdot mol $^{-1}$ for ROOH, which is twice as high as the O–O BDE (39.549–41.655 kcal \cdot mol $^{-1}$). Therefore, the homolytic cleavage of the O–O bond of ROOH occurs easily in absence of metal co-catalysts at the beginning or at low temperature, leading to the rapid generation of PINO \cdot by the reaction of the NHPI with the formed RO \cdot . It should also be noted that the O–O BDE of ROOH in the polar solvents is lower than that of ROOH in the apolar solvents due to their favorable intermolecular hydrogen-bonding interactions, which is evident from the cyclohexane oxidation studies and UV–visible spectra characterization (Fig. 2). Furthermore, one can conclude that the more nucleophilic the RO \cdot (from the NBO charge) in CH $_3$ CN is, the higher reaction reactivity toward NHPI it has, an assertion which is also supported by the spin density distributions.

In a catalytic cycle, the key elementary steps for the one-step oxidation of cyclohexane to AA are summarized sequentially below [32]: (i) first, one C–H bond of the cyclohexane is activated by the PINO \cdot ; and (ii) second, one α -C–H bond of the cyclohexanone intermediates is activated by the same PINO \cdot . By focusing on the rate-limiting step, the free energy barriers of the two types of H-abstraction (cyclohexane and cyclohexanone) respectively are calculated by B3LYP functionals. IRC calculations show that such elementary steps proceed through H-bonded pre- and post-reaction complexes, resulting in a substantial depression of the transition state energy as depicted in Fig. 4, in which the precise relative energies of the pre- and post-reaction complexes are of significant influence in different solvents. Fig. 4 indicates that the H-abstraction process of cyclohexane can be divided into two processes: C–H bond approaching PINO \cdot and the breaking of C–H bonds. At the beginning, the pre-reaction complex that is formed between the reactants has an activated structure with the longer C–H distance (see Table 4). Relative to the separated reactants, the fairly strongly bound pre-reaction complexes in the gas phase

have free energies of 5.2497 kcal \cdot mol $^{-1}$. However, the inclusion of estimates of the solvent effects increases the endergonicity of pre-reaction complex formation to 7.5891 kcal \cdot mol $^{-1}$ in CH $_3$ CN, 5.9563 kcal \cdot mol $^{-1}$ in benzene and 5.9299 kcal \cdot mol $^{-1}$ in cyclohexane. As we know, the pre-reaction complex is first formed between the reactants by H-abstraction, in which the proton and electron are thought to be transferred by different molecular orbitals: a C–H hydrogen as a proton to a δ -lone pair on the PINO \cdot oxygen and the electron from a 2p-s orbital on the cyclohexane to the 2p singly occupied orbital on the PINO \cdot oxygen. However, it is very likely that the proton transfer is not yet complete with the occurrence of the electron jump at the pre-reaction complexes state, resulting in a charge imbalance whereby a partial positive charge resides in the cyclohexane moiety and a partial negative charge on the PINO \cdot oxygen, thus nicely accounting for a more efficient stabilization by the solvent. On this basis, it was not surprising that, in aerobic cyclohexane oxidations catalyzed by NHPI without metal cocatalyst, CH $_3$ CN is an excellent solvent, in view of the presence of the electron-donating nitrogen atom (Fig. 6). Further, the thermodynamic quantity involved in the enthalpy of the pre-reaction complex gives an important insight into the active participation of solvent molecule. The value obtained for the enthalpy of the pre-reaction complex in CH $_3$ CN (0.6350 kcal \cdot mol $^{-1}$) is significantly lower than those in the gas phase (1.0492 kcal \cdot mol $^{-1}$) or apolar solvents (1.1534 kcal \cdot mol $^{-1}$ for cyclohexane; 1.1684 kcal \cdot mol $^{-1}$ for benzene). This indicates that pre-reaction complex in CH $_3$ CN with stronger hydrogen bonds are the preferred.

Similar trends in the cases of the cyclohexanone pre-reaction complex abstracted by PINO \cdot in different solvents are also observed in the computational modeling (Fig. 5 and Table 5). This beneficial effect of the CH $_3$ CN solvent molecule can be directly attributed to the increased stabilization of the pre-reaction complex in solution, due to its ability to form strong hydrogen bonds. In addition, the values for this beneficial effect were also calculated from those determined for the enthalpy of the cyclohexanone pre-reaction complex. The enthalpy is 0.3175 kcal \cdot mol $^{-1}$ kcal \cdot mol $^{-1}$ in CH $_3$ CN, which is obviously lower than those in the apolar solvents (1.5587 kcal \cdot mol $^{-1}$ for cyclohexane; 1.3692 kcal \cdot mol $^{-1}$ for benzene) or gas phase (3.4701 kcal \cdot mol $^{-1}$). The TS structures of cyclohexane associated with the HAT reaction of PINO \cdot with cyclohexane are found to exhibit a “cisoid” structure with the anti-bonding interactions for O \cdots H \cdots C systems (Fig. 4). The free energy of the TS structure in polar CH $_3$ CN is 28.3367 kcal \cdot mol $^{-1}$, slightly higher than those in the gas phase or apolar solvents (28.0208–28.3208 kcal \cdot mol $^{-1}$). As in the above discussion, the polar contribution of the solvents with the formation of a hydrogen-bond plays an important role in the HAT reactivity of N-oxyl radicals with an ability to stabilize the positive and negative charges developing in the TS (Table 4).

After the HAT process is completed, the free energies associated with complexation within the post-reaction complex of

Table 3
O–H, O–O bond lengths and bond dissociation energies, atomic spin densities and NBO charges for ROOH, ROO \cdot and RO \cdot in various solvents.

Solvent	ROOH (R–O $_2$ –O $_1$ –H)				ROO \cdot (R–O $_2$ –O $_1$)		RO \cdot (R–O $_2$)	
	O $_1$ –H	O $_1$ –O $_2$	BED O $_1$ –H	BED O $_1$ –O $_2$	p O $_1$	SD_{O_1}	p O $_2$	SD_{O_2}
Gas	0.96581	1.45310	86.016	41.655	–0.183	0.681491	–0.328	0.849042
Acetone	0.96780	1.45045	86.449	39.603	–0.213	0.656562	–0.370	0.835486
Acetic acid	0.96740	1.45088	86.297	39.891	–0.212	0.660803	–0.362	0.830268
Acetonitrile	0.96789	1.45037	86.486	39.549	–0.219	0.655707	–0.372	0.824469
Propionitrile	0.96786	1.45039	86.475	39.565	–0.218	0.655960	–0.372	0.824771
Benzonitrile	0.96784	1.45041	86.466	39.578	–0.218	0.656165	–0.371	0.825015
Pyridine	0.96769	1.45056	86.404	39.676	–0.216	0.657578	–0.368	0.826802
Cyclohexane	0.96663	1.45229	86.078	40.699	–0.197	0.671843	–0.344	0.840564
Benzene	0.96661	1.45140	86.099	40.575	–0.200	0.668575	–0.347	0.839281

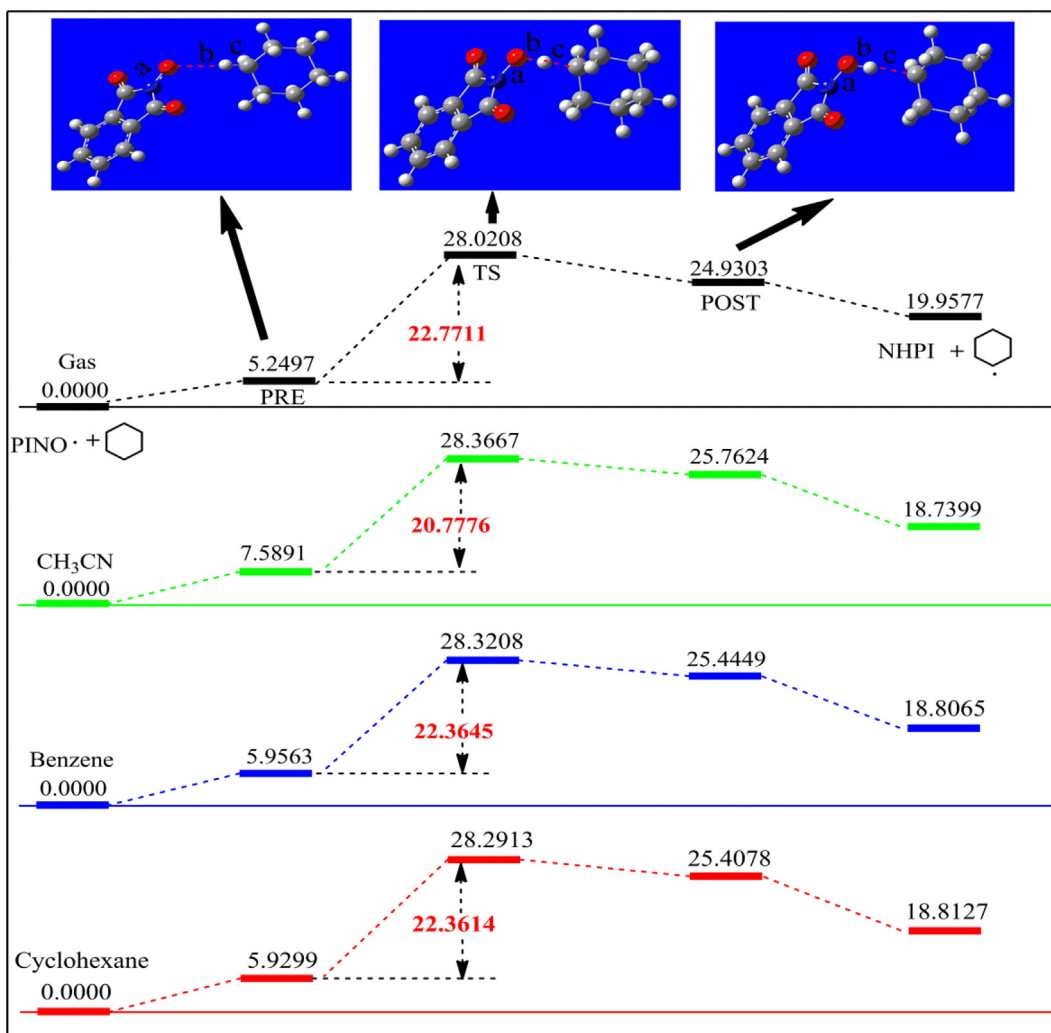


Fig. 4. The relative free energy ($\text{kcal}\cdot\text{mol}^{-1}$) of the cyclohexane + PINO \cdot reaction in various solvent media; PRE, TS, and POST refer to pre-complex, transition state, and post-complex, respectively.

Table 4

The most relevant geometrical parameters and atomic spin densities (SD) for the H-abstraction of PINO \cdot from cyclohexane. PRE, TS, and POST refer to pre-complex, transition state, and post-complex, respectively.

PINO \cdot + Cyclohexane		Atomic distance ^a			Spin density			
		a N ₁ –O ₂	b O ₂ –H ₃	c H ₃ –C ₄	SD _N	SD _O	SD _{H1}	SD _{C4}
Gas	PRE	1.26465	2.80686	1.09738	0.236757	0.609196	-0.001042	0.001863
	TS	1.34433	1.16384	1.40432	0.031098	0.013145	0.007624	0.636895
	POST	1.37172	0.99539	1.99979	0.028216	-0.013109	0.054421	0.999824
Acetonitrile	PRE	1.26502	2.87216	1.09818	0.272754	0.575925	-0.000874	0.002299
	TS	1.34659	1.18239	1.39398	0.033524	0.240111	0.026386	0.609703
	POST	1.37183	1.00137	1.97347	0.029006	-0.019307	0.068700	0.975234
Benzene	PRE	1.26472	2.89192	1.09766	0.251024	0.596686	-0.000860	0.001493
	TS	1.34506	1.17328	1.39778	0.031329	0.250937	0.015414	0.623725
	POST	1.37196	0.99770	1.99361	0.029857	-0.017122	0.060518	0.989071
Cyclohexane	PRE	1.26470	2.89117	1.09762	0.249082	0.598470	-0.000865	0.001457
	TS	1.34494	1.17220	1.39844	0.031246	0.251642	0.014405	0.625240
	POST	1.37190	0.99746	1.99362	0.029797	-0.016658	0.059821	0.989892

^a Along with the definition of atomic distances (a–c) and the most relevant atoms (N₁, O₂, H₃, C₄, and C₅) during the H-abstraction process.

cyclohexane are calculated to be 25.7624 kcal·mol⁻¹ in polar CH₃CN, but a slightly lower value is observed both in gas phase and apolar solvents. The free energies of the final dissociated products of the HAT reaction in polar solvent are 18.7399 kcal·mol⁻¹ (CH₃CN) lower than those of the apolar solvent (Fig. 4). The calculations

predict that the reaction species involved in the oxidation process will not remain complexed in polar solvents. A similar change for free energies of the post-reaction complex and final dissociated products in the cyclohexanone HAT reaction is observed in different solvents; nevertheless the free energies of the post-reaction

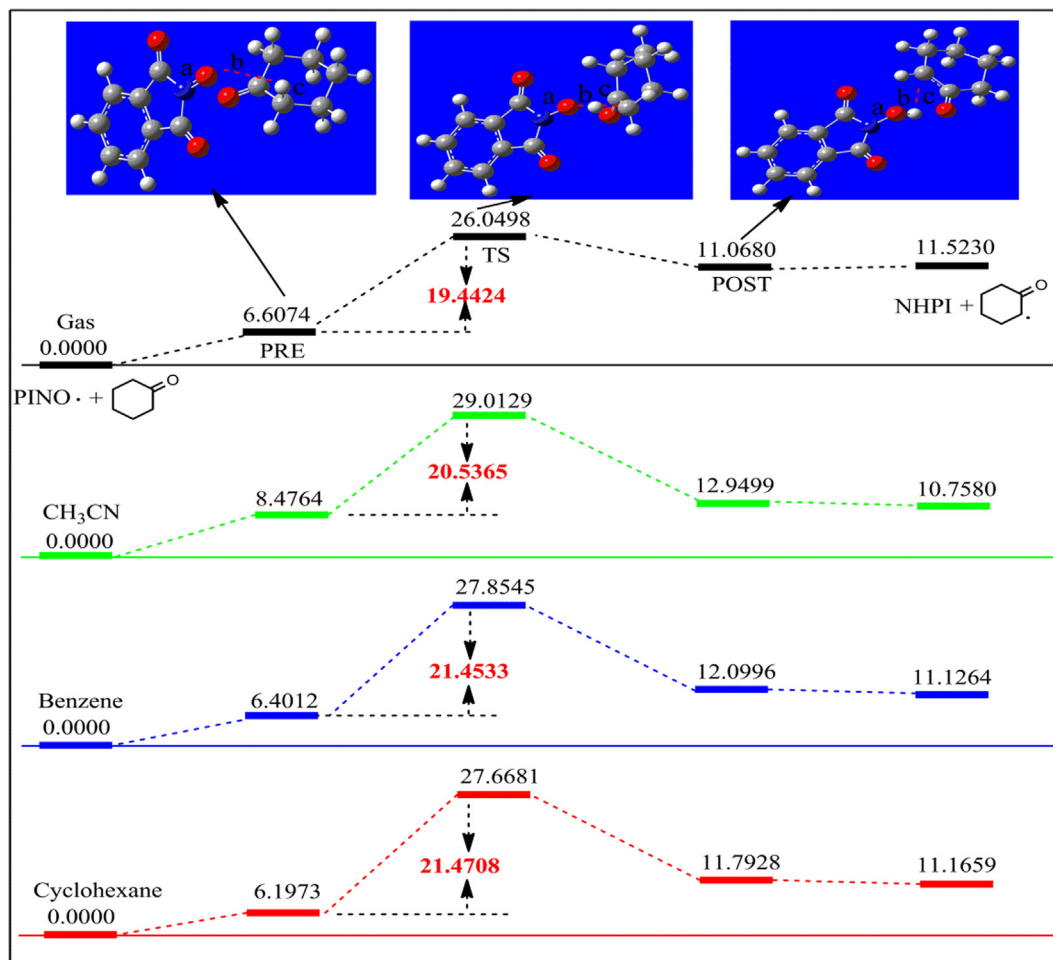


Fig. 5. The relative free energy ($\text{kcal}\cdot\text{mol}^{-1}$) of the cyclohexanone + $\text{PINO}\cdot$ reaction in various solvent medium; PRE, TS and POST refer to pre-complex, transition state and post-complex, respectively.

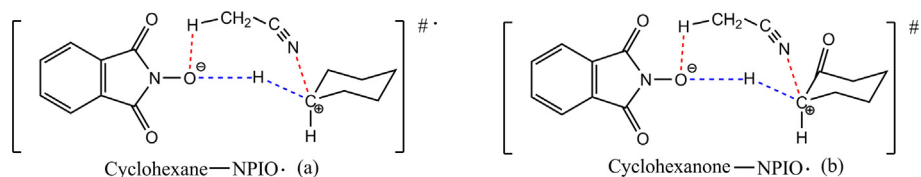


Fig. 6. Suggested models of the limit transition state structure for the reaction of $\text{PINO}\cdot$ with cyclohexane (a) and cyclohexanone (b) depending on the charge balance of solvent-interactions.

complex are close to the free energies of final dissociated products, which indicates that the reaction of $\text{PINO}\cdot$ + cyclohexanone will be much faster than the reaction of $\text{PINO}\cdot$ with the C–H bond of cyclohexane. Additionally, the reactivity of $\text{PINO}\cdot$ in the HAT processes is also clearly dependent on the enthalpic requirements of the C–H bond dissociation energies and a degree of charge transfer in TS state by means of the polar effect of the solvents that may stabilize the activated complex [48,49]. Thus, the pre-reaction complexes show higher free energies due to the stabilization of the positive and negative charges by the polar solvent, which lowers the reaction energy barrier further (from $28.3667 \text{ kcal}\cdot\text{mol}^{-1}$ to $20.7776 \text{ kcal}\cdot\text{mol}^{-1}$, Fig. 4) for cyclohexane oxidation in CH_3CN , resulting in a high reactivity. Combining the calculated energy barrier with the catalytic data, we find that the higher reactivity of cyclohexanone than of the cyclohexane can be attributed to the lower energy barrier ($20.5365 \text{ kcal}\cdot\text{mol}^{-1}$ vs $20.7776 \text{ kcal}\cdot\text{mol}^{-1}$, Fig. 5), which could explain the much higher AA selectivity.

3.5. Possible synergistic reaction mechanisms

As the data above show, for the one-step oxidation of cyclohexane by dioxygen, reaction in polar solvents does not show any catalytic activity under our conditions, NHPI has only a slight catalytic effect with the production of organic peroxide, and very interestingly the combination of CH_3CN and NHPI exhibits a high catalytic ability towards the one-step product AA. To further understand the catalytic reaction mechanism of the metal-free catalytic system, several additional experiments are carried out. At first, 4 mol% hydroquinone as a free radical scavenger was added into the NHPI-based catalytic oxidation system with CH_3CN as solvent, and no cyclohexane oxidation occurred. This indicates that the process follows a radical mechanism. Secondly, $\text{Mn}(\text{OAc})_2$ as a metal co-catalyst was used to add the above NHPI- CH_3CN catalytic system under the same conditions, and it only gave a negative effect with slightly low cyclohexane conversion (22.8%) and AA

Table 5

The most relevant geometrical parameters and atomic spin densities (SD) for the H-abstraction of PINO[•] from cyclohexanone. PRE, TS and POST refer to pre-complex, transition state and post-complex, respectively.

PINO [•] + Cyclohexanone		Atomic distance ^a			Spin density			
		a N ₁ –O ₂	b O ₂ –H ₃	c H ₃ –C ₄	SD _N	SD _O	SD _{H1}	SD _{C4}
Gas	PRE	1.26386	3.05681	1.10128	0.246834	0.061381	–0.000238	–0.000191
	TS	1.33285	1.18403	1.38352	0.087383	0.281199	–0.030118	0.517669
	POST	1.37020	0.99796	2.97739	–0.001442	0.002344	–0.004259	0.807531
Acetonitrile	PRE	1.26423	4.75777	1.10099	0.276015	0.566994	0.000029	–0.001171
	TS	1.33383	1.19382	1.38274	0.081012	0.279100	–0.023910	0.506226
	POST	1.37111	1.00494	3.01565	–0.000414	0.002028	–0.004424	0.802950
Benzene	PRE	1.26386	3.73062	1.10115	0.257171	0.584397	0.000031	–0.000546
	TS	1.33326	1.18896	1.38221	0.084133	0.281318	–0.027209	0.512370
	POST	1.37040	1.00078	3.00299	–0.001452	0.002377	–0.004318	0.805292
Cyclohexane	PRE	1.26385	3.64715	1.10116	0.255564	0.585663	0.000016	–0.000663
	TS	1.33321	1.18835	1.38230	0.084230	0.281463	–0.027536	0.512981
	POST	1.37039	1.00045	2.99433	–0.001477	0.002395	–0.004312	0.805312

^a Along with the definition of atomic distances (a–c) and the most relevant atoms (N₁, O₂, H₃, C₄, and C₅) during the H-abstraction process.

selectivity (70.3%), which implied that CH₃CN plays a key role in the formation of AA (Table 1, entry 13). Also in this case, the addition of tiny amounts of CH₃CN (equimolar ratios with the NHPI unit) resulted in a significant increase in cyclohexane or reaction intermediates (cyclohexanone and cyclohexanol) conversion, from trace levels to 6.8% (Table S1, entry 4, 10 and 11), confirming again the active participation of the polar solvent molecule for NHPI-catalytic oxidation. Additionally, characterizations such as UV–visible spectroscopy and voltammetry are carried out to clarify the synergistic HAT for solvent effect. Distinctly identifiable spectra of NHPI are observed in different solvents by UV–vis; meanwhile, the homolytic cleavage of the O–O bond of ROOH to form a radical initiator for NHPI can be strongly accelerated in the presence of the hydrogen-bond interaction with solvent. These experimental observations are quite in line with their BDEs and H-abstraction barriers of PINO[•] in the corresponding solvent derived from DFT calculations.

Transition metal ions such as Co²⁺/3⁺ and Mn²⁺/3⁺ are often added to the cyclohexane oxidation reaction, because they are known to catalyze the initiation reaction [50,51]. In our metal-free catalytic systems (Fig. 7), the homolytic dissociation of RO–OH, with the assistance of the solvent H-bonded interaction is responsible for first chain initiation by heating due to its 50% lower RO–OH BDE (about 39 kcal·mol^{–1}) than the H–O BDE for NHPI (about 84 kcal·mol^{–1}). The next step contains the radical exchange between NHPI and ·OH/RO[•], and the resulting N-oxyl radical of protonated NHPI has a better H-abstraction ability [49], which can abstract a hydrogen atom from cyclohexane to form cyclohexyl radical more easily with the pre-reaction complexes due to the lower energy barrier through the solvent-effect (20.7776 kcal·mol^{–1} for CH₃CN, 22.7711 kcal·mol^{–1} for gas-phase conditions, 22.3645 kcal·mol^{–1} for benzene, 22.3614 kcal·mol^{–1} for cyclohexane self). Importantly, it is crucial to the catalysis process that N-oxyl radical don't terminate with each other or with peroxy radicals, which is a much more efficient chain carrier than ROO[•]/RO[•] with enhanced radical chain length [52,53]. The next elementary step is that the cyclohexyl radical is easily captured by O₂ to generate peroxy radical, which is converted to ROOH through its H-abstraction from >NO–H bond of NHPI [54]. Then, the polar solvents by means of hydrogen-bonded interactions help to decompose ROOH into ketone products. In addition, the obtained cyclohexyl radicals are highly reactive, followed by addition of an ·OH to form a cyclohexanol. Generally, the BDE value of the C–H bond R₂C(OH)–H in cyclohexanol (92.4 kcal/mol) is lower than that of the C–H bonds in the α position (94.1 kcal/mol) in cyclohexanone intermediate [37], meaning that the formed cyclohex-

anol is further oxidized more easily with the production of ·OH at the weakest methine C–H bond to form a geminal diol (1,1'-dihydroxycyclohexane) [55]. Geminal diols are well-known to be very unstable and will rapidly undergo dehydration to product stable cyclohexanone [24,56].

As emphasized in another key elementary step, α-H abstraction from cyclohexanone is also a very important reaction in determining the formation of the AA product. Therefore, the reactivity of PINO[•] toward cyclohexanone is evaluated in different solvents. Based on the above computed energy barriers for α-H abstraction in CH₃CN solvent from cyclohexane and cyclohexanone by PINO[•] (20.7776 kcal·mol^{–1} and 20.5365 kcal·mol^{–1}, respectively), we can estimate that the free PINO[•] species react faster with cyclohexanone than cyclohexane. Thus, the H-abstraction at the carbon adjacent to the oxygen in cyclohexanone can most likely be promoted in the presence of polar solvents due to the π-overlap between the C=O groups of cyclohexanone and PINO[•], with preferential stabilization of the TS structures. The production of ketonyl radical at this α C=O position readily leads to the formation of ketonyl hydroperoxide with oxygen, which can be decomposed into a ketonyl radical with the assistance of the polar solvents. Ultimately, the ketonyl hydroperoxide radical is stabilized by the solvent CH₃CN to a great extent, then reacts to yield the radical species OHC–(CH₂)₄–C(O[•]) by the ring opening via C–C scission; successive oxidation steps lead to the formation of AA. Alternatively, the production of the ketonyl radical can also be captured by reactive ·OH to the formation of 2-hydroxycyclohexanone, which may undergo a pathway to generate hydroxy-lactone with further oxidation to form acid anhydride, followed by hydrolysis to produce AA [57]. The above reaction mechanism is supported by reaction intermediates detection during the course of the reaction. Separate experiments confirm that hydroxy-lactone can be converted to AA under the same condition.

4. Conclusion

Generally, the role of solvent is limited to the simple requirement for diluting and/or dissolving reactants in the liquid-phase catalytic reactions. Here, insights are presented into the influence of solvents (acetone, acetic acid, acetonitrile, benzonitrile, propionitrile, pyridine and benzene) on manipulation of the catalytic activity and AA selectivity for one-step aerobic oxidation of cyclohexane catalyzed by NHPI catalysts under promoter- and metal-free conditions. We found that a polar solvent molecule actively participates in production of PINO[•] from NHPI for crucial reaction

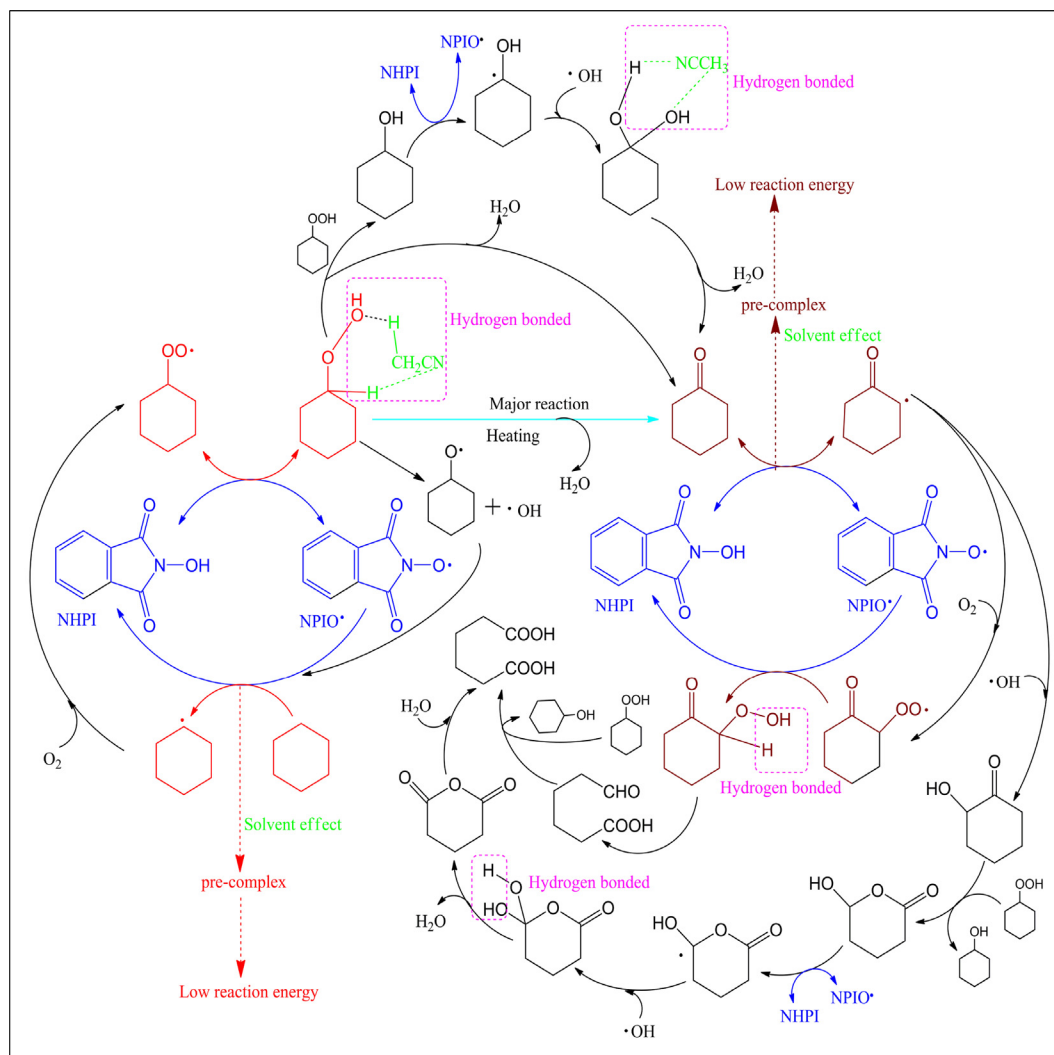


Fig. 7. Mechanistic pathway for oxidative conversion of cyclohexane to AA.

steps and significantly affects the catalytic behavior, which is confirmed by using the cyclic voltammetry measurements combined with UV–vis spectra techniques. In order to systematically elucidate the active role of the solvent, DFT calculations coupled with a continuum solvation model (PCM) are carried out to investigate the electronic properties of NHPI and intermediates, and the barriers involved in the two types of H-abstraction on PINO• sites in the different solvent environments. Our calculations show that the solvent-polarity changes the electronic properties of NHPI and intermediates significantly. The transition state barrier of H-abstraction for cyclohexane decreases from 22.36 (in benzene) to 20.78 kcal·mol⁻¹ (in acetonitrile), whereas the α -H-abstraction barrier for cyclohexanone decreases from 21.45 to 20.53 kcal·mol⁻¹. The calculated results suggest that the catalytic oxidation of cyclohexane and cyclohexanone intermediate represents a strong case of active solvent participation, which consists of assisting the rate-determining H-abstraction process by forming pre-reaction complex and nicely accounting for a more efficient stabilization with favorable intermolecular hydrogen-bonding interactions by the polar solvents; the hydrogen atom transfer via PINO•••H•••C< process is thereby considerably accelerated. Meanwhile, modeling of solvent effects predicts that cyclohexanone oxidation pathways are favored over cyclohexane oxidation pathways. Thus, acetonitrile is the best solvent for the one-step oxidation of cyclohexane to AA: a conversion of 28% with 79% AA

selectivity is achieved over NHPI catalysts. This work provides a novel mechanism of the solvent effect for designing a new class of metal-free molecular switches that are active in different solvent environments.

Acknowledgments

This work was supported by the Natural Science Foundation of China (Grant No. 21576078, 21878074 and 21978078) and the Natural Science Foundation of Hunan Province (Grant No. 2016JJ2081) and Innovation Platform Open Fund of Hunan College (16K052) and Collaborative Innovation Center of New Chemical Technologies for Environmental Benignity and Efficient Resource Utilization.

Appendix A. Supplementary material

Supplementary data to this article can be found online at <https://doi.org/10.1016/j.jcat.2019.08.042>.

References

- [1] E. Roduner, W. Kaim, B. Sarkar, V.B. Urlacher, J. Pleiss, R. Gläser, W.-D. Einicke, G.A. Sprenger, U. Beifus, E. Klemm, C. Liebner, H. Hieronymus, S.F. Hsu, B. Plietker, S. Laschat, *ChemCatChem* 5 (2013) 82–112.
- [2] G. Qian, D. Ji, G. Lu, R. Zhao, Y. Qi, J. Suo, *J. Catal.* 232 (2005) 378–385.

- [3] G. Huang, L.Q. Mo, J.L. Cai, X. Cao, Y. Peng, Y.A. Guo, S.J. Wei, *Appl. Catal. B: Environ.* 162 (2015) 364–371.
- [4] Y.R. Luo, CRC Press (2007).
- [5] K. Sato, M. Aoki, R. Noyor, *Science* 281 (1998) 1646–1647.
- [6] B.P.C. Hereijgers, B.M. Weckhuysen, *J. Catal.* 270 (2010) 16–25.
- [7] J. Dai, W. Zhong, W. Yi, M. Liu, L. Mao, Q. Xu, D. Yin, *Appl. Catal. B: Environ.* 192 (2016) 325–341.
- [8] C. Davies, K. Thompson, A. Cooper, S. Golunski, S.H. Taylor, M.B. Macias, O. Doustdar, A. Tsolakis, *Appl. Catal. B: Environ.* 239 (2018) 10–15.
- [9] M.J. Gilkey, A.V. Mironenko, D.G. Vlachos, B. Xu, *ACS Catal.* 7 (2017) 6619–6634.
- [10] L. Zhao, B. Pudasaini, A. Genest, J.D. Nobbs, C.H. Low, L.P. Stubbs, M. Meurs, N. Rösch, *ACS Catal.* 7 (2017) 7070–7080.
- [11] K. Tanaka, *Chemtech* 4 (1974) 555–559.
- [12] M. Costantini, E. Fache, US Patent CN6147256, 2000.
- [13] D. Bonnet, T. Ireland, E. Fachea, J.P. Simonato, *Green Chem.* 8 (2006) 556–559.
- [14] H. Lü, W. Ren, P. Liu, S. Qi, W. Wang, Y. Feng, F. Sun, Y. Wang, *Appl. Catal. A: Gen.* 441 (2012) 136–141.
- [15] M. Dugal, G. Sankar, R. Raja, J.M. Thomas, *Angew. Chem. Int. Ed.* 112 (2000) 2399–2402.
- [16] G. Zou, W. Zhong, Q. Xu, J. Xiao, C. Liu, Y. Li, L. Mao, S. Kirk, D. Yin, *Catal. Commun.* 58 (2015) 46–52.
- [17] Y. Ishii, *J. Mol. Catal. A: Chem.* 117 (1997) 123–137.
- [18] H. Yu, F. Peng, J. Tan, X. Hu, H. Wang, J. Yang, W. Zheng, *Angew. Chem. Int. Ed.* 50 (2011) 3978–3982.
- [19] Y.H. Cao, X.Y. Luo, H. Yu, F. Peng, H.J. Wang, G.Q. Ning, *Catal. Sci. Technol.* 3 (2013) 2654–2660.
- [20] P. Tang, G. Hu, M. Li, D. Ma, *ACS Catal.* 6 (2016) 6948–6958.
- [21] X. Wang, Y. Li, *J. Mater. Chem. A* 4 (2016) 5247–5257.
- [22] R.A. Sheldon, I.W.C.E. Arends, *Adv. Synth. Catal.* 346 (2004) 1051–1071.
- [23] R. Amorati, M. Lucarini, V. Mugnaini, G.F. Pedulli, *J. Org. Chem.* 68 (2003) 1747–1754.
- [24] P.J. Figiel, J.M. Sobczak, *J. Catal.* 263 (2009) 167–172.
- [25] A. Dhakshinamoorthy, M. Alvaro, H. Garcia, *J. Catal.* 289 (2012) 259–265.
- [26] I. Hermans, J.V. Deun, K. Houthoofd, J. Peeters, P.A. Jacobs, *J. Catal.* 251 (2007) 204–212.
- [27] M. Zhao, X.-W. Zhang, C.D. Wu, *ACS Catal.* 7 (2017) 6573–6580.
- [28] I. Hermans, P. Jacobs, J. Peeters, *Phys. Chem. Chem. Phys.* 9 (2007) 686–690.
- [29] C. Einhorn, J. Einhorn, C. Marcadal, J.-L. Pierre, *Chem. Commun.* 5 (1997) 447–448.
- [30] O. Fukuda, S. Sakaguchi, Y. Ishii, *Adv. Synth. Catal.* 343 (2001) 809–813.
- [31] Z. Du, Z. Sun, W. Zhang, H. Miao, H. Ma, J. Xu, *Tetrahedron Lett.* 50 (2009) 1677–1680.
- [32] M. Petroselli, L. Melone, M. Cametti, C. Punta, *Chem. Eur. J.* 23 (2017) 10616–10625.
- [33] T. Iwahama, K. Syojyo, S. Sakaguchi, Y. Ishii, *Org. Process Res. Dev.* 2 (1998) 255–260.
- [34] M.J. Frisch et al., *Gaussian 09* (2009).
- [35] K. Chen, H. Xie, K. Jiang, J. Mao, *Chem. Phys. Lett.* 657 (2016) 135–141.
- [36] M. Petroselli, P. Franchi, M. Lucarini, C. Punta, L. Melone, *ChemSusChem* 7 (2014) 2695–2703.
- [37] F. Recupero, C. Punta, *Chem. Rev.* 107 (2007) 3800–3842.
- [38] G.W. Parshall, S.D. Ittel, *Homogeneous Catalysis*, Wiley, 1992.
- [39] N. Koshino, B. Saha, J.H. Espenson, *J. Org. Chem.* 68 (2003) 9364–9370.
- [40] Y. Zhang, W. Dai, G. Wu, N. Guan, L. Li, *Chin. J. Catal.* 35 (2014) 279–285.
- [41] M. Salamone, M. Bietti, *Synlett* 25 (2014) 1803–1816.
- [42] F. Minisci, F. Recupero, A. Cecchetto, C. Gambarotti, C. Punta, R. Paganelli, *Org. Process Res. Dev.* 8 (2004) 163–168.
- [43] G.J. Suppes, M.A. McHugh, *Ind. Eng. Chem. Res.* 28 (1989) 1146–1152.
- [44] Y. Ishii, S. Sakaguchi, *Catal. Today* 117 (2006) 105–113.
- [45] D. Serve, *Electrochim. Acta* 20 (1975) 469–477.
- [46] K. Gorgy, J.-C. Lepretre, E. Saint-Aman, C. Einhorn, J. Einhorn, C. Marcadal, J.-L. Pierre, *Electrochimica Acta* 44 (1998) 385–393.
- [47] C. Annunziatini, P. Baiocco, M.F. Gerini, *J. Mol. Catal. B: Enzym.* 32 (2005) 89–96.
- [48] F. Minisci, C. Punta, F. Recupero, F. Fontana, G.F. Pedulli, *Chem. Commun.* 7 (2002) 688–689.
- [49] C. D'Alfonso, M. Bietti, G.A. DiLabio, O. Lanzalunga, M. Salamone, *J. Org. Chem.* 78 (2013) 1026–1037.
- [50] G. Franz, R.A. Sheldon, *Oxidation*, *Ullmann's Encyclopedia of Industrial Chemistry*, 2000.
- [51] S.A. Chavan, D. Srinivas, P. Ratnasamy, *J. Catal.* 212 (2002) 39–45.
- [52] I. Hermans, L. Vereecken, P.A. Jacobs, J. Peeters, *Chem. Commun.* 9 (2004) 1140–1141.
- [53] J.E. Nutting, M. Rafiee, S.S. Stahl, *Chem. Rev.* 118 (2018) 4834–4885.
- [54] L. Melone, C. Punta, *Beilstein J. Org. Chem.* 9 (2013) 1296–1310.
- [55] K.C. Hwang, A. Sagadevan, *Science* 346 (2014) 1495–1498.
- [56] I. Ignatyev, M. Montejo, P.G.R. Ortega, J.J.L. González, *Phys. Chem. Chem. Phys.* 13 (2011) 18507–18515.
- [57] S.-O. Lee, R. Raja, K.D.M. Harris, J.M. Thomas, B.F.G. Johnson, G. Sankar, *Angew. Chem.* 115 (2003) 1558–1561.